

Formation of metastable ferroelectric clusters in $\text{K}_{1-x}\text{Li}_x\text{Ta}_{1-y}\text{Nb}_y\text{O}_3:\text{Cu,V}$ at the paraelectric phase

Gabby Bitton, Meir Razvag, and Aharon J. Agranat

Department of Applied Physics, The Hebrew University of Jerusalem, Jerusalem 91904, Israel

(Received 5 January 1998)

We present experimental evidence indicating that in potassium lithium tantalate niobate at the paraelectric phase, ferroelectric clusters are formed to compensate the space charge induced field created in a photorefractive process. These clusters are distributed in a slow spontaneous process and form a dipolar grating which is spatially correlated with the photorefractive space charge grating. By investigating the Gibbs free energy, we show that the compensating gratings are formed only in the temperature region where a metastable ferroelectric state is allowed to exist at the paraelectric phase. The compensation process, as well as its temperature and electric field dependence are interpreted in terms of the Gibbs free energy. [S0163-1829(98)04633-5]

I. INTRODUCTION

It was recently reported¹⁻³ that in paraelectric potassium lithium tantalate niobate (KLTN) crystals, slightly above the phase transition temperature, stable dipolar clusters are formed in response to the creation of a photorefractive space charge. Specifically it was observed² that within a certain temperature range above the phase transition, the diffraction efficiency of holograms that are left to dwell in the dark immediately after the writing process, evolves with time according to the electric field applied to the crystal. In these experiments,² first, a volume hologram was written on a KLTN crystal in the presence of an external electric field E_W , then the crystal was left to dwell in the dark under an applied electric field E_D . It was observed that when E_D was parallel to E_W the diffraction efficiency decreased slowly during the dwell period. After the dwell period the hologram was illuminated by a diffused light beam with the same wavelength used for writing under zero external electric field. It was observed that during this erasure phase the diffraction efficiency decreased exponentially to zero. Following the erasure phase, the application of an external electric field caused the diffraction efficiency to recover to a substantial fraction of its original value. This phenomenon was attributed to a slow spontaneous formation of a dipolar grating that compensates the regular photorefractive (PR) grating. It was further shown¹ that the dipolar grating originated from local changes in the dc dielectric permittivity ϵ , which in the presence of an external uniform electric field, induced changes in the low frequency polarization of the form $\delta P \propto \delta\epsilon E$. Moreover, in the region where the Curie-Weiss law is applicable (i.e., where the mean field approximation is valid), the changes in the dc dielectric permittivity $\delta\epsilon$ were found to originate from local changes in the Curie-Weiss temperature T_0 .

The PR effect is normally attributed to the formation of a spatially modulated space charge, which causes a correlated modulation in the birefringence through the electrooptic effect.⁴ At the paraelectric phase, the electrooptic effect is quadratic, and hence the electric field induced birefringence is given by

$$\Delta n(\mathbf{r}) = \frac{1}{2} n_0^3 g_{\text{eff}} P_{\text{tot}}^2, \quad (1)$$

where n_0 is the refractive index, g_{eff} is the effective electrooptical coefficient, and P_{tot} is the (dc or low frequency) polarization induced by the internal electric field. The polarization could be separated into two parts $P_{\text{tot}} = P_0 + \delta P(\mathbf{r})$ where P_0 is the polarization induced by internal uniform electric field and $\delta P(\mathbf{r})$ is the spatially variable component of the polarization created by the PR process. In terms of P_0 and δP the induced birefringence is given by

$$\Delta n(\mathbf{r}) = \frac{1}{2} n_0^3 g_{\text{eff}} [P_0^2 + 2P_0 \delta P(\mathbf{r}) + \delta P(\mathbf{r})^2]. \quad (2)$$

The first term in the brackets is a spatially uniform change in the birefringence. If the spatial dependence of $\delta P(\mathbf{r})$ results from the interference of two planar waves propagating in directions \mathbf{K}_1 and \mathbf{K}_2 , respectively, it is given by $\delta P(\mathbf{r}) = A + B \cos(\mathbf{K} \cdot \mathbf{r})$, where A and B are constants and \mathbf{K} is the wave vector of the grating given by $\mathbf{K} = \mathbf{K}_1 - \mathbf{K}_2$. In this case the second term in Eq. (2) is proportional to $\cos(\mathbf{K} \cdot \mathbf{r})$, where the third term is proportional to $\cos^2(\mathbf{K} \cdot \mathbf{r})$. Since our measurements are performed with a probe beam which is incident at an angle that matches the Bragg condition for a \mathbf{K} grating the first and the third terms are irrelevant. Therefore the probe beam is diffracted by a grating given by

$$[\Delta n(\mathbf{r})]_1 = n_0^3 g_{\text{eff}} P \delta P(\mathbf{r}). \quad (3)$$

In a regular PR process, the polarization grating $\delta P(\mathbf{r})$, originates exclusively from the created space charge [i.e., $\delta P(\mathbf{r}) = \epsilon E_{\text{sc}}(\mathbf{r})$]. When the dipolar clusters are formed, the induced birefringence is given by

$$\Delta n(\mathbf{r}) = n_0^3 g_{\text{eff}} \epsilon^2 E_0 E_{\text{sc}}(\mathbf{r}) - n_0^3 g_{\text{eff}} \epsilon \delta\epsilon(\mathbf{r}) E_0^2, \quad (4)$$

where ϵ is the dielectric constant, $\delta\epsilon(\mathbf{r})$ is the dipolar grating in terms of the spatial variations created in ϵ , E_0 is the internal dc field in the crystal, and $E_{\text{sc}}(\mathbf{r})$ is the spatial variations in the internal field induced by the PR space charge. The first term on the right side is the contribution of the

space charge created in the PR process and the second term is the contribution of the dipolar clusters which compensate for the space charge grating and is given a minus sign for empirical reasons.

Consider the case of two plane waves interfering in the crystal. The formed grating is of the form $\Delta n(\mathbf{r}) = \Delta n_0 + \Delta n_1 \cos(\mathbf{k} \cdot \mathbf{r})$. The diffraction efficiency of such a grating is given by⁵

$$\eta = e^{-\alpha d} \sin^2 \left(\frac{\pi \Delta n_1 d}{\lambda_R \cos \theta} \right), \quad (5)$$

where λ_R is the wavelength of the reading beam, α is the absorption coefficient at λ_R , θ is the angle between the wave vector of the reading beam and the normal to the grating vector, d is the thickness of the material, and it is assumed that the reading beam matches the Bragg condition. Thus, local polarization changes that are formed during the compensation process can be studied by monitoring the diffraction efficiency of the induced grating.

In this paper an experimental investigation of the temperature and electric field dependence of both the dipolar compensation process and the Gibbs free energy (GFE) function will be presented. The observed dependence of the compensation process on temperature and electric field will be explained in terms of the GFE function for a first order phase transition which was found to occur in the crystals under investigation.

II. EXPERIMENTAL RESULTS

Investigations of the compensation process as a function of the applied electric field and the temperature for two $\text{K}_{1-x}\text{Li}_x\text{Ta}_{1-y}\text{Nb}_y\text{O}_3\text{:Cu,V}$ crystals (crystal *A* with $x = 0.005$, $y = 0.13$, and $T_c = 136.7$ K, and crystal *B* with $x = 0.006$, $y = 0.173$, and $T_c = 168$ K) were carried out. The electric field dependence of the compensation process in crystal *A* was measured for several different electric fields. In all experiments a hologram was recorded in the crystal under the same conditions. Two plane wave beams with intensities of 25 mW/cm^2 were incident on the crystal with an incidence angle of 9.5° and -9.5° . The writing period lasted 7 sec during which an electric field of 1.8 kV/cm was applied. The holograms were then left to dwell in the dark under an applied electric field. In all but one experiment this electric field was equal and parallel to the writing field, whereas in one experiment the electric field was equal in magnitude but anti parallel to the writing field. During the dwell period the diffraction was monitored using a He-Ne laser (the detailed experimental setup is described in Ref. 2). The diffraction efficiency as a function of time is shown in Figs. 1 and 2. As can be seen in Fig. 1 when a positive (with respect to the writing field) electric field was applied during the dwell period a slow decrease in the diffraction efficiency was observed, whereas when a negative electric field was applied during the dwell period a relatively fast increase in the diffraction efficiency was observed. In Fig. 2 the time evolution of the diffraction efficiency during the dwell period is shown for several amplitudes of the applied electric field ($E = 1.8, 1.45, 1.1, 0.73 \text{ V/cm}$). As can be seen a faster decrease in the diffraction efficiency is observed when the applied electric field is stronger.

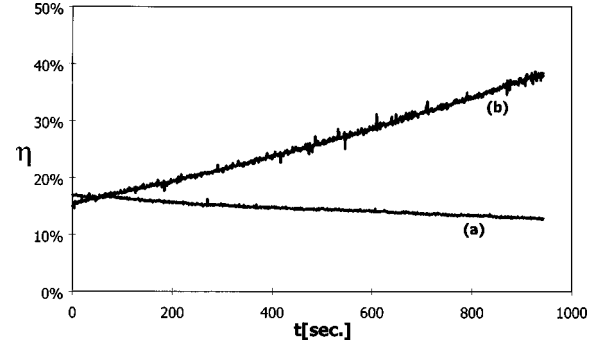


FIG. 1. The time evolution of the diffraction efficiency under different applied electric fields for a grating recorded in crystal *B* at $T_c + 4$ K. (a) Under an applied electric field parallel and equal in magnitude to the writing field. (b) Under an applied electric field antiparallel and equal in magnitude to the writing field.

The temperature dependence of the compensation process was investigated in crystal *B*. The diffraction efficiency was measured as a function of time for four different temperatures $T = T_c + 1 \text{ K}$, $T_c + 2 \text{ K}$, $T_c + 3 \text{ K}$, $T_c + 4 \text{ K}$. In each of the above temperatures a hologram was written at the same conditions described above (i.e., exposure time of 7 sec, beam intensity of 25 mW/cm^2 , incidence angle of the beams 9.5° and -9.5° , applied electric field strength of 1.8 kV/cm). It was then left to dwell under a positive electric field of 1.8 kV/cm applied in parallel to E_w for 15 min during which the diffraction efficiency was monitored using a He-Ne laser. Figure 3 shows the time evolution of the diffraction efficiency for the above temperatures. It can be seen the decrease in the diffraction efficiency became faster as the temperature approached the phase transition temperature.

In order to have a better understanding of the effect of the electric field and temperature on the compensation process, we investigated the dependence of the GFE function on these two parameters. The GFE functions of crystals *A* and *B* were computed from measurements of the constant dielectric permittivity as function of electric field for different temperatures. The constant dielectric permittivity was measured at a low frequency of 130 Hz. The method of computation is standard,^{6,7} and involves the evaluation of the polarization as function of electric field and temperature through the given relation:

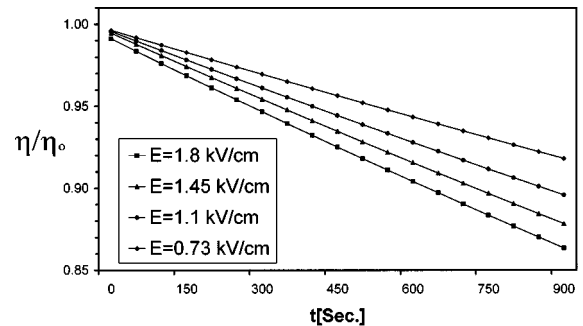


FIG. 2. The time evolution of the diffraction efficiency under four applied electric fields for a grating recorded in crystal *B* at $T_c + 4$ K: (a) $E_D = 1.8 \text{ kV/cm}$, (b) $E_D = 1.45 \text{ kV/cm}$, (c) $E_D = 1.1 \text{ kV/cm}$, (d) $E_D = 0.73 \text{ kV/cm}$. (η_0 is the diffraction efficiency immediately after writing, and the applied field is parallel to the writing field.)

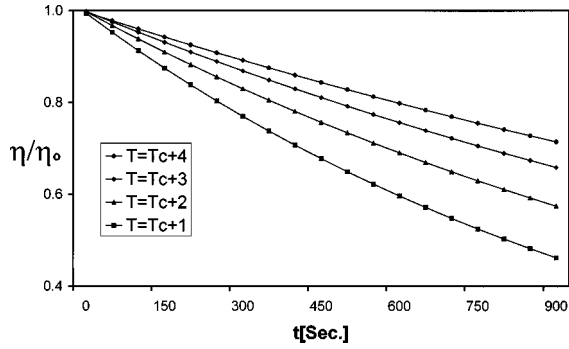


FIG. 3. The time evolution of the diffraction efficiency at four temperatures of a grating recorded in crystal *B* under an applied electric field of 1.8 kV/cm: (a) $T = T_c + 1$ K, (b) $T = T_c + 2$ K, (c) $T = T_c + 3$ K, (d) $T = T_c + 4$ K.

$$P(E) = P(0) + \varepsilon_0 \int_0^E \varepsilon dE, \quad (6)$$

where it was assumed that $P(0)$ could be neglected above the phase transition and special care was taken to ensure that inner bias fields were taken into account. The measured polarization can be used to determine the GFE function since its value is a minimum of this function.

In general, the GFE function for a ferroelectric material is given by

$$g(P, T) = g_0 + \frac{\alpha}{2} P^2 + \frac{\gamma}{4} P^4 + \frac{\delta}{6} P^6 - EP, \quad (7)$$

where α, γ, δ are temperature-dependent parameters.

The temperature dependence of the parameter α is approximated in the region where the mean field approximation is valid by $\alpha = \beta(T - T_0)$, where $\beta = 1.4 \times 10^5$ J m/(C² K) and $T_0 = 163$ K. The temperature dependence of γ was fitted to a linear function of the form $\gamma(T) = A(T - T_2)$, where $A = 2.4 \times 10^6$ J m⁵/(C⁴ K) and $T_2 = 174.6$ K. The fact that γ has a negative value below T_2 indicates that the transition is first order. The parameter δ is given by $\delta = 2.45 \times 10^6$ J m⁹/C⁶.

The four temperatures T_0, T_1, T_2 , and T_c , which were derived from the GFE function, define different states of the crystal. Consider Fig. 4 where the computed GFE of crystal

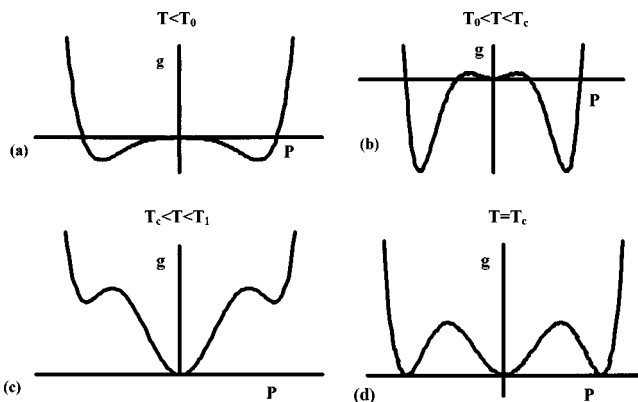


FIG. 4. The Gibbs free energy function of crystal *A* vs the polarization at four different temperatures with no external electric field: (a) $T < T_0$, (b) $T_0 < T < T_c$, (c) $T_1 < T < T_c$, (d) $T = T_c$.

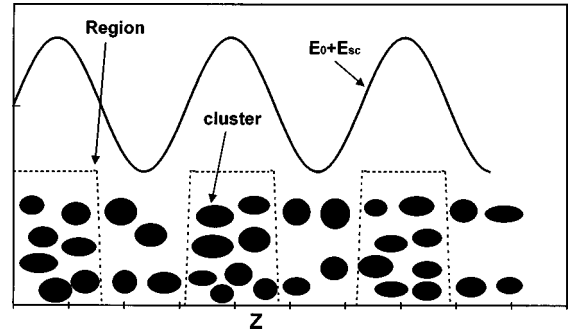


FIG. 5. Schematic description of the ferroelectric clusters distribution according to the local electric field inside the crystal.

B is plotted for four different temperatures: $T_0 = 163$ K, $T_1 = 169.5$ K, $T_2 = 174.6$ K, and $T_c = 167$ K. For $T < T_0$ [Fig. 4(a)], the minima of the GFE function are at nonzero polarization points. For $T_c > T > T_0$ [Fig. 4(b)], a local minimum at $P = 0$ exists in addition to the two global minima at $P \neq 0$. This situation is reversed for $T_1 > T > T_c$ [Fig. 4(c)], where the two minima at $P \neq 0$ become local minima and the minimum point at $P = 0$ becomes the global minimum. For $T > T_1$ only the minimum at $P = 0$ exists. However, for $T_2 > T > T_1$ a minimum point at $P \neq 0$ can be induced by applying an external electric field. Whereas for $T > T_2$ the minimum point at $P = 0$ remains the only minimum point regardless of the strength of the applied field. The interesting result is that the temperature range where the compensation process occurred, and the irregular dipolar grating appeared has been identified as $[T_c, T_2]$, where T_2 is the highest temperature at which an external electric field can induce a ferroelectric state and T_c is the phase transition temperature. We can extract two more parameters from the free energy function, the spontaneous polarization at the phase transition temperature $P_{sc} = 0.3$ [C/m²], and the dependence of the phase transition temperature on the applied electric field $dT_c/dE = 8.4 \times 10^{-5}$ [K m V⁻¹]. Note that the result that was obtained directly from a measurement of the dielectric constant is $dT_c/dE = 3 \times 10^{-5}$ [K m V⁻¹].

III. DISCUSSION

The key finding described in the previous section is the fact that the occurrence of the dipolar grating formation is limited to the temperature range $[T_c, T_2]$, where metastable ferroelectric clusters are allowed to exist in the paraelectric phase in the presence of an electric field. It is therefore reasonable to assume that the dipolar grating consists of such ferroelectric clusters which are formed in response to the space charge induced field. A qualitative description of the clusters formation process is presented in Fig. 5. The spatial variations in the internal electric field inside the crystal are induced by the space charge that is formed in the PR process. These variations of the local electric field cause the formation of correlated variations in the relative distribution between the ferroelectric and paraelectric states of small volume elements in the crystal. Thus, in each region of the crystal, ferroelectric clusters are created and redistributed in a slow spontaneous process with size and abundance which depend on the local electric field. These ferroelectric clusters, which are spatially correlated with the space charge induced

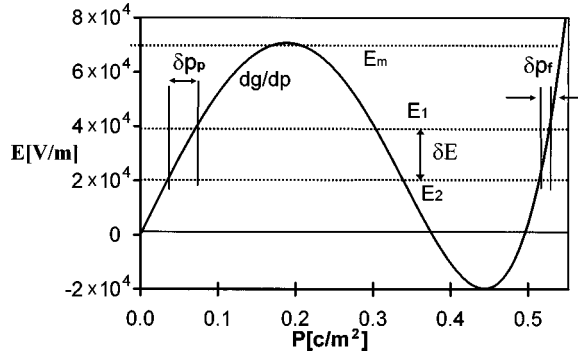


FIG. 6. Evaluation of the (meta)stable points of the polarization of crystal B at $T = T_c + 0.5$ K by a graphic solution of $\partial g / \partial P = y(P) - E = 0$. Note that for $E > E_M$ only the ferroelectric solution exists, whereas for $E < E_M$ the system has both a paraelectric and a ferroelectric solutions.

field, form the compensating dipolar grating.

The dependence of the clustering process on electric field and temperature can be explained by the GFE function. Consider the GFE function for the temperature range $[T_c, T_2]$. As pointed out above, at this temperature range a metastable ferroelectric state can coexist together with the paraelectric state in the presence of an electric field. The probability for finding the system in a certain polarization P is given by⁸

$$W[P] = A \exp\{[g(P) - g_0] / k_B T\}, \quad (8)$$

where $g(P)$ and g_0 are the densities of the GFE for the polarization P and for the paraelectric state, respectively, and A is a normalization constant. Thus, the probability depends on the difference between the free energy for a system with a given polarization P and the free energy of the paraelectric phase. In general, the system resides most of the time in the minima of the GFE. These minima can be extracted from the first derivative of the GFE density given by

$$\partial g / \partial P = (\alpha + \gamma P^2 + \delta P^4)P - E = y(P) - E = 0. \quad (9)$$

A graphic solution of $\partial g / \partial P = 0$ for crystal A in the temperature range $[T_c, T_2]$ is presented in Fig. 6. As can be seen for $E = 0$ three minima occur at $P_p = 0$ and at $P_F = \pm P_0$. For a certain value of the internal electric field E , two minima occur at $P_p = \varepsilon_p E$ and at $P_F = P_0 + \varepsilon_F E$, where ε_p and ε_F are the small signal dielectric permittivity (i.e., $\varepsilon = \delta P / \delta E$) at $P = 0$ and $P = P_0$, respectively.

The effective small signal dielectric permittivity is given by

$$\varepsilon_{\text{eff}} = \delta P / \delta E = (1 - x)\varepsilon_p + x\varepsilon_F, \quad (10)$$

where x designates the relative distribution between the paraelectric and ferroelectric states (i.e., between the minima of g , at P_p and P_F , respectively). In terms of Eq. (8), during the dipolar grating formation process the value of x changes, and the formed dipolar grating originates from changes in ε_{eff} . Thus, in terms of ε_{eff} the grating of the ferroelectric clusters can be described as the dielectric grating described in Ref. 1.

The electric field inside the crystal can be described by $E(z) = E_0 + E_1 \sin(z/\lambda)$, where E_0 is the amplitude of the dc component of the field and E_1 is the amplitude of the spa-

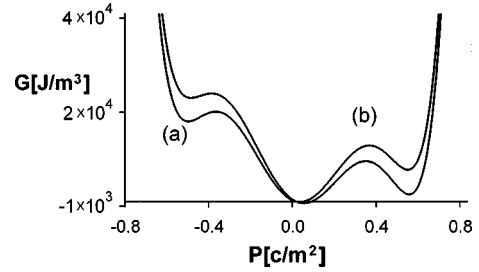


FIG. 7. The Gibbs free energy function of crystal B at $T = T_c + 1$ K is plotted for two different electric fields $E(a) = 2E(b)$.

tially dependent component of the field. E_0 is the combined contribution of the applied field and the dc component of the space charge induced field and E_1 is the fundamental spatial frequency component of the space charge induced field. A straightforward computation of the amplitude of the space charge field immediately after the writing (before the compensating grating is formed, i.e., for $\delta\varepsilon = 0$), based on Eqs. (1)–(3) and the data in Ref. 2, reveals that $E_1 \approx 40$ V/cm, while $E_0 \approx 1.1$ kV/cm. As pointed out above, E_1 triggers the formation of the dipolar grating. Note that $E_1 \ll E_0$ and yet the formation of the dipolar cluster is very effective. This is primarily due to the fact that the relative distribution between the P_p and P_F is an exponential function of E [see Eq. (8)]. In addition, the dc component E_0 has an amplifying effect. Consider first Figs. 7(a) and 7(b) where the free energy function of crystal A at $T = T_c + 1$ K is plotted for two different electric fields. It is evident from Fig. 7 that increasing E_0 causes the ferroelectric minimum of the GFE to become deeper, and consequently the effect of increasing E_0 is to amplify the effect of E_1 . Thus, the onset of the dipolar compensating grating is faster, and the formed grating is more effective as E_0 is increased. These predictions are in accord with the data presented in Fig. 2 showing the buildup of the dipolar grating during a positive dwell stage for several different values of E_0 . It should be noted that if E_0 exceeds the limiting value E_M above which only the ferroelectric minimum of the GFE exists (see Fig. 6) the compensating grating can no longer be formed. The dc component of the space charge induced field created during the PR writing stage is antiparallel to the applied field. Accordingly, the dc component of the space charge induced field and the electric field applied during either the positive or negative dwell processes (designated above by E_D), are either antiparallel or parallel, respectively. In the experiments described above, the contribution to the dc component to the electric field from the space charge induced field had a typical value of about 700 V/cm, hence, the dc part of the electric field during positive dwell process was about 1.1 kV/cm while the dc part of the electric field in the negative dwell was about 2.5 kV/cm. Thus, in these experiments E_0 was significantly smaller than E_D during the “positive” dwell processes, while during the “negative” dwell E_0 was significantly larger than E_D . We assume for the latter case that it was larger than E_M so that the dipolar grating was not formed. We attribute the increase in the diffraction that was observed during the negative dwell to a global increase of ε_{eff} .

The temperature dependence of the dipolar clusters formation process is presented in Fig. 3 and the compensation rate becomes faster as the phase transition temperature is

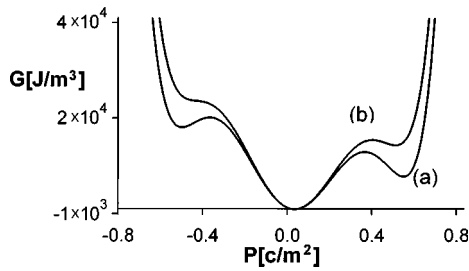


FIG. 8. The Gibbs free energy of crystal B is plotted for two different temperatures: (a) $T = T_c + 0.5$ K and (b) at $T = T_c + 1$ K.

approached. This result is in agreement with the result presented in Fig. 8 where the GFE function is plotted for two different temperatures within $[T_c, T_2]$, for the same electric field. It can be seen that the energy gap between the ferroelectric state and the paraelectric state decreases as $T \rightarrow T_c$. The time evolution of the diffraction efficiency in Fig. 3 can be fitted using the following relation:

$$[\delta(\Delta n)]^2 \propto \eta = \eta_0 e^{-t/\tau}, \quad (11)$$

where η_0 is the initial diffraction efficiency and τ is the lifetime of the recorded hologram. Usually the lifetime of similar processes which involve thermal excitation can be fitted to the classical Arrhenius relation. We found here that only Vogel-Fulcher law⁹ gives a reasonable fit. The Vogel-Fulcher law is characteristic of systems where the energy gap depends on system parameters and is given by

$$1/\tau = (1/\tau_0) \exp\{E'_a/[k_B(T - T_f)]\}, \quad (12)$$

where τ is a characteristic life time, T_f is normally referred to as the freezing temperature, and E'_a is the activation energy. This activation energy is related to the actual activation energy which depends on the system parameters through the following relation:¹⁰ $E_a = E'_a T/(T - T_f)$. From the fitted data we find that $T_f = 170$ K. That is, T_f coincides with the temperature at which the maximum in the dielectric permittivity under an electric field of 1.8 kV/cm is obtained. Recall that the electric field applied for the data presented in Fig. 3 is also 1.8 kV/cm. The fact that the temperature dependence of the time evolution of the dipolar clusters formation process follows a Vogel-Fulcher law indicates that it is implicitly dependent on the applied field through T_f .

In summary, we have shown the existence of a spontaneous formation of ordered structures of dipolar clusters slightly above the first order phase transition in KLTN crystals. The formed structures are spatially correlated to local variations in the internal electric field created during the recording of holograms by a PR process. The rate of creation and stability of the dipolar clusters which form the structures are very sensitive to both the applied field and the temperature. The dipolar clusters are stable only within a temperature range where metastable ferroelectric state is allowed in the paraelectric phase.

ACKNOWLEDGMENTS

This research was supported in part by The Israel Science Foundation founded by the Israel Academy of Science & Humanities and by the Ministry of science of the state of Israel.

¹A. J. Agranat, M. Razvag, M. Balberg, and G. Bitton, Phys. Rev. B **55**, 12 818 (1997).

²A. J. Agranat, M. Razvag, M. Balberg, and V. Leyva, J. Opt. Soc. Am. B **14**, 2043 (1997).

³A. J. Agranat, M. Razvag, and M. Balberg, Appl. Phys. Lett. **68**, 2469 (1996).

⁴N. V. Kukhtarev V. B. Mrkov, S. G. Odulov, M. S. Soskin, and L. Vinetskii, Ferroelectrics **22**, 949 (1979).

⁵R. J. Collier, *Optical Holography* (Academic, New York, 1971), Chap. 9, p. 247.

⁶M. E. Lines and A. M. Glass, *Principles and Applications of Ferroelectrics and Related Materials* (Clarendon, Oxford,

1977), pp. 59–81.

⁷E. Fatuzzo and W. J. Merz, *Ferroelectricity*, edited by E. P. Wohlfath (North-Holland, Amsterdam, 1967), pp. 105–135.

⁸R. Blinc and B. Zeks, *Soft Modes in Ferroelectric and Antiferroelectrics*, edited by E. P. Wohlfath (North-Holland, Amsterdam, 1974), pp. 34–35.

⁹H. Vogel, Phys. Z. **22**, 645 (1921).

¹⁰A. S. Kewitsch, M. Segev, A. Yariv, G. J. Salamo, T. W. Towe, E. J. Sharp, and R. R. Neurgaonkar, Phys. Rev. Lett. **73**, 1174 (1994).